International Journal of Concrete Structures and Materials
Vol.1, No.1, pp.45~55, December 2007

Glass FRP-Bonded RC Beams under Cyclic Loading

Kiang-Hwee Tan[1)]* and Mithun-Kumar Saha[2)]

(Received August 10, 2007, Accepted November 26, 2007)

Abstract : Ten beams bonded with glass fiber reinforced polymer (GFRP) laminates were tested under cyclic loading with the load range and the FRP reinforcement ratio as test parameters. The maximum load level during cyclic loading was 55%, 65% and 75% of the static flexural strength while the minimum load level was kept constant at 35%. Deflections of the beams at the end of 525000 cycles were found to increase by 16% and 44% when the maximum load level was increased from 55% to 65% and 75% of the static flexural strength, respectively. Beams with FRP reinforcement ratios of 0.64% and 1.28% were found to exhibit lesser deflections of about 15% and 20%, respectively, compared to a similar beam without FRP reinforcement. An analytical approach based on cycle-dependent effective moduli of elasticity of concrete and FRP reinforcement is presented and found to predict the deflections of the test beams well.

Keywords : beams, cyclic loading, deflection, glass fiber reinforced polymer, stiffness

1. Introduction

The use of fiber reinforced polymer (FRP) composite laminates in strengthening bridge structures has become popular, primarily due to the higher strength-weight ratio and easier installation of the material compared to other conventional materials like steel plates. For such structures, the behavior under cyclic loading is of concern. A number of studies had been performed on carbon FRP (CFRP)-strengthened structures under cyclic loading to date.[1-4] Most of these studies dealt with the increase in fatigue life of the structures due to externally bonded CFRP laminates, without considering the effect on the deformation of the structures. However, as deflections are expected to increase with cyclic loading, the serviceability of such structures may be compromised.

The issue of serviceability of CFRP-bonded RC beams under cyclic loading has been addressed in some studies. Breña et al.[3] discussed the cumulative deflection and strain due to cyclic loading and concluded that beams subjected to load amplitudes corresponding to service-load conditions in a bridge, did not exhibit significant accumulation of damage up to one million cycles. On the other hand, beams subjected to extreme load conditions in a bridge showed significant deterioration and failed during cyclic loading. In another study on pre-cracked RC beams, Wu et al.[4] found that in beams that were subjected to cyclic loads within the service load level up to a maximum of two million cycles, the CFRP laminates had bridging effects on cracks, the propagation of which was considered as the main reason for the stress change in steel rebars and reduction in beam stiffness. However, for beams subjected to larger load ranges, the CFRP laminates showed crack restraining properties only up to 300,000 cycles after which cracks were found to widen significantly.

In the present study, uni-directional glass FRP (GFRP)-bonded RC beams were subjected to cyclic loads of different amplitudes and their deformation characteristics are evaluated. An analytical approach is also presented to calculate the deflections of external FRP-bonded RC beams under cyclic loading.

2. Research significance

The present study investigates the deformation characteristics of GFRP-bonded RC beams under cyclic loading. The beam stiffness was found to reduce more significantly for larger load ranges and lower minimum load levels. Deflections of the beams increase with an increase in the load range, while they decrease with an increase in FRP reinforcement ratio. The improved behavior in deflection was found to be in tandem with the flexural strength enhancement. An analytical method is also presented to compute the deflections of FRP-bonded RC beams under cyclic loading, and it was found to predict the experimental results well.

3. Test program

The test program is shown in Table 1. A total of ten beams were tested, nine of which were bonded with GFRP laminates. To facilitate comparison, the program was divided into two series. In Series I, the beams were tested to examine the effect of load range, ΔP, while in Series II, they were tested to investigate the effect of FRP reinforcement ratio, ρ_{frp}. The load range, ΔP, is defined as the difference between the maximum (P_{max}) and minimum (P_{min}) applied loads during the cyclic loading, while

[1)]Dept. of Civil Engineering, National University of Singapore, Singapore 117576. *E-mail: cvetankh@nus.edu.sg*
[2)]CB&I Lummus Pte Ltd., Singapore.

Table 1 Test program

	Beam designation	ρ_{frp},%	P_{min}, kN (kips)	P_{max}, kN (kips)	$\overline{\sigma_m}$ (Eq. 3)	$\overline{\Delta\sigma}$ (Eq. 4)	Remarks
Series I (Effect of Load Range, ΔP^*)	C11	0.64	0.35 P_0, 9.4 (2.11)	0.55P_0, 14.8 (3.33)	0.38	0.17	P_{max} as test parameter; P_{min}/P_0 = 0.35 ρ_{frp} = 0.64%
	C12	0.64		0.65P_0, 17.5 (3.93)	0.42	0.25	
	C13	0.64		0.75P_0, 20.2 (4.53)	0.46	0.34	
	C11a	0.64	0.35 P_1, 11.2 (2.51)	0.55P_1, 17.6 (3.96)	0.45	0.20	P_{max} as test parameter; P_{min}/P_1 = 0.35; ρ_{frp} = 0.64%
	C12a	0.64		0.65P_1, 20.8 (4.67)	0.50	0.30	
	C13a	0.64		0.75P_1, 24.0 (5.39)	0.55	0.40	
	C21b	1.28	0.35 P_2, 12.5 (2.81)	0.55 P_2, 19.6 (4.40)	0.47	0.21	P_{max} as test parameter; P_{min}/P_2 = 0.35; ρ_{frp} =1.28%
	C22b	1.28		0.65 P_2, 23.2 (5.21)	0.52	0.31	
Series II (Effect of FRP Reinforcement Ratio, ρ_{frp})	C02	0	0.35 P_0, 9.4 (2.11)	0.65 P_0, 17.5 (3.93)	0.46	0.27	ρ_{frp} as test parameter; $\Delta P/P_0$ = 0.30
	C12	0.64			0.42	0.25	
	C22	1.28			0.39	0.24	
	C02	0	0.35 P_0, 9.4 (2.11)	0.65 P_0, 17.5 (3.93)	0.46	0.27	ρ_{frp} as test parameter; $\Delta P/P_u$ = 0.30
	C12a	0.64	0.35 P_1, 11.2 (2.51)	0.65 P_1, 20.8 (4.67)	0.50	0.30	
	C22b	1.28	0.35 P_2, 12.5 (2.81)	0.65 P_2, 23.2 (5.21)	0.52	0.31	
	C11a	0.64	0.35 P_1, 11.2 (2.51)	0.55 P_1, 17.6 (3.96)	0.45	0.20	ρ_{frp} as test parameter; $\Delta P/P_u$ = 0.20
	C21b	1.28	0.35 P_2, 12.5 (2.81)	0.55 P_2, 19.6 (4.40)	0.47	0.21	

* $\Delta P = P_{max} - P_{min}$

the FRP reinforcement ratio, ρ_{frp}, is defined as the FRP reinforcement area divided by the gross concrete area in a cross-section.

The beams are in general, designated as CXYs. The symbol 'X' denotes the number of layers of GFRP laminates; with '0' indicating no GFRP (that is, ρ_{frp}= 0%), '1' for one layer of GFRP laminate (ρ_{frp}= 0.64%), and '2' for two layers of GFRP laminate (ρ_{frp}= 1.28%). The symbol 'Y' describes the load range. The load ranges were selected by considering that in practice, dead load contributes to about 40%, while live load contributes the remaining 60% of the total load on a structural member. A member can be subjected to a load combination ranging from "full dead load plus one-third live load" to "full dead load plus full live load" in its life time. By incorporating a load factors of 1.4 and 1.7 respectively for dead and live loads for ultimate load capacity, the lower and upper load levels translate respectively to 35% and 65% of the static ultimate load capacity (P_u) of the member.

In this study, the lower load level was taken as 35% of P_u while the upper load level was varied as 55%, 65%, and 75%. The value of '1' in place of 'Y' indicates the case where the load was varied from 35% to 55% of P_u, '2' for 35% to 65% of P_u, and '3' for 35% to 75% of P_u. The value of P_u is defined by the suffix "s"; blank for P_0, "a" for P_1, and "b" for P_2, where P_0, P_1, and P_2 are the static flexural capacities of RC beams with ρ_{frp} of 0%, 0.64%, and 1.28%, respectively. The load was applied at a constant frequency of 2 Hz for up to a maximum of 525,000 cycles. The number of cycles was limited to 525,000 cycles as the degradation in structural performance was significant only in the first thousand cycles or so.

3.1 Material properties

A concrete mix proportion of 1 : 1.96 : 2.6 by the weight of Ordinary Portland Cement, natural sand and crushed granites of 10 mm (3/8 in.) nominal size was used to cast the beams. The cement content was 394 kg/m^3 (24.62 lb/ft^3) and the water-cement ratio was 0.53. The concrete cube compressive strength at 28 days was found to be about 42 MPa (6.09 ksi), while the modulus of elasticity and modulus of rupture were about 25 GPa (3,625 ksi) and 5 MPa (0.725 ksi), respectively. Two types of reinforcement bars were used in the beams: hot-rolled deformed high yield bars, 6 (1/4 in.) and 10 mm (3/8 in.) in diameters (designated as T6 and T10, respectively), and plain round mild steel bars, 6 mm (1/4 in.) in diameter (designated as R6). The average yield strength was 525 MPa (76.1 MPa), 520 MPa (75.4 MPa), and

212 MPa (30.74 ksi) and modulus of elasticity was 183 (26535), 194 (28130), and 200 GPa (29,000 ksi) for T6, T10, and R6 bars, respectively.

Uni-directional E-glass fiber sheet was used with a two-part, 100% solid, low viscosity amine cured epoxy to form the GFRP laminates of about 0.8 mm (0.0315 in.) thickness per layer. The properties of glass fiber sheets and resin, as supplied by the manufacturer, are shown in Table 2. Primer was used according to the manufacturer's instructions to prepare the beam surface for proper bonding of the GFRP laminates.

3.2 Specimen details

All beams measured 100 × 125 mm (3.94 × 4.92 in.) in cross-section and 2,000 mm (78.74 in.) in total length as shown in Fig. 1. Two T10 bars were used as tensile reinforcement and placed at a depth of 99 mm (3.90 in.) whereas two T6 bars were used as compressive reinforcement and placed at 24 mm (0.94 in.) from the top face of the beam. R6 stirrups were placed at a spacing of 75 mm (2.95 in.) throughout the entire length of the beams. All beams were covered with wet gunny sacks for 7 days after casting and then left to dry under ambient laboratory condition. To eliminate the effect of shrinkage and ageing of concrete on deformation, the beams were tested three months after casting. However, the GFRP system was installed 21 days after casting using the wet lay-out procedure. To facilitate bonding of the glass fiber sheets, the tension soffits of the beams were mechanically ground. At the cut-off points of the GFRP system near the end of the span, a fiber sheet of 100 mm (3.94 in.) width was attached transversely over the specimens to prevent premature plate-end debonding of the GFRP system.

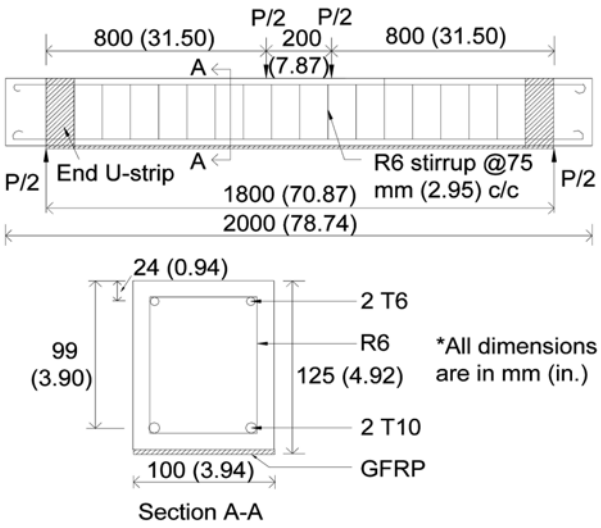

Fig. 1 FRP-bonded RC beams and section properties.

3.3 Test set-up and instrumentation

The beams were simply supported over a span of 1,800 mm (70.87 in.). Loads were applied at two points distant 200 mm (7.87 in.) apart and symmetrically placed about the mid-span, as shown in Fig. 2. Instrumentation of the beams is shown in Fig. 3. Strain gauges of 5 mm (0.20 in.) length were mounted on the tensile steel bars at mid-span before casting of beams. Strain gauges of 30 mm (1.18 in.) length were also installed at the mid-span on the top concrete face and on the GFRP reinforcement for each beam.

Deflections were measured at mid-span, beneath the two loading points and at quarter points using linear variable displacement transducers (LVDTs) during static loading, and at mid-span and beneath the two loading points using potentiometric displacement transducers during cyclic loading. The LVDTs were connected to the data logger whereas the potentiometric displacement transducers were connected to an oscilloscope to record the data. The complete deformation characteristics were recorded during the 1st, 10th, 100th, 1,000th, 5,000th, 10,000th, 25,000th, 50,000th, 75,000th, 175,000th, 200,000th, 225,000th, 250,000th, 350,000th, 400,000th, and 525,000th cycles.

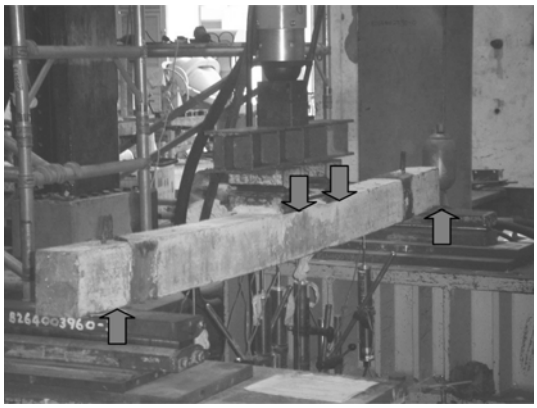

Fig. 2 Test set-up.

Table 2 Fiber and resin properties.

Fiber	Type	E-glass
	Sheet form	Unidirectional roving
	Fiber areal weight density, g/m^2 (lbs/ft^2)	915 (0.19)
	Design thickness, mm/ply (in./ply)	0.353 (0.014)
	Tensile strength, MPa (ksi)	1700 (246.50)
	Modulus of elasticity, GPa (ksi)	71 (10295)
	Ultimate strain, %	2
Resin	Type	Two part, 100% solid, low viscosity amine cured epoxy
	Tensile strength, MPa (ksi)	54 (7.83)
	Modulus of elasticity, GPa (ksi)	3 (435)
	Ultimate strain, %	2.5

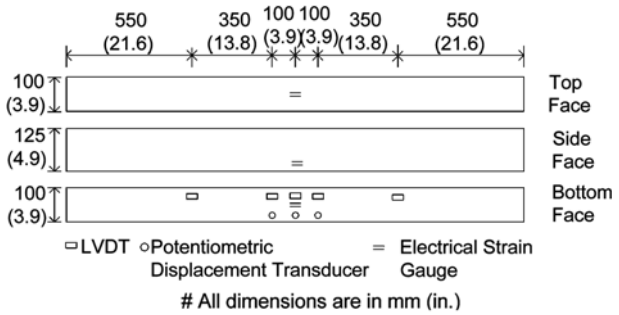

Fig. 3 Instrumentation of beams.

4. Analytical considerations

4.1 Factors affecting deflections under cyclic loading

The increase in deflections of FRP-bonded RC beams under cyclic loading can be attributed to: (i) the cyclic creep of concrete in the compression zone, (ii) the decrease in tensile stiffening of concrete with increased cracking, and (iii) the cyclic softening of FRP in tension. From available results for metals and thin wires[5], it is assumed that steel reinforcement bars are cyclically stable at working load levels.

4.2 Cyclic creep of concrete in compression

Creep strain of concrete in the compression zone under cyclic loading is found to be a significant factor for the increased deflections of beams. To account for cyclic creep, an effective cycle-dependent secant modulus of elasticity of concrete, $E_{e,N}$ is considered, that is[5]:

$$E_{e,N} = \frac{\sigma_{\max}}{\frac{\sigma_{\max}}{E_c} + \varepsilon_{c,N}} \tag{1}$$

where N = number of cycles, $\sigma_{\max}$ = average stress in concrete at the maximum load level, E_c = static modulus of elasticity of concrete, and $\varepsilon_{c,N}$ = cyclic creep strain in concrete which consists of a mean strain component resulting from the static mean stress and a cyclic strain component which depends on the stress range,[6] that is:

$$\varepsilon_{c,N} = 129\,\overline{\sigma}_m(1 + 3.87\Delta\overline{\sigma})t^{\frac{1}{3}} \tag{2}$$

where t = time after the beginning of cyclic loading in hours. It is noted that cyclic load tests were conducted on specimens at a frequency rate of about 9.75 Hz in establishing Eq. (2).

In Eq. (2), $\overline{\sigma}_m$ and $\overline{\Delta\sigma}$ are both non-dimensional terms, defined as:

$$\overline{\sigma}_m = \frac{\sigma_m}{f_c'} = (\sigma_{\max} + \sigma_{\min})/(2f_c') \tag{3}$$

$$\overline{\Delta\sigma} = \frac{\Delta\sigma}{f_c'} = (\sigma_{\max} - \sigma_{\min})/(f_c') \tag{4}$$

where $\sigma_{\min}$ = average stress in concrete at the minimum load level, and f_c' = 28-day concrete cylinder compressive strength. For a beam under flexural loading, both $\sigma_{\max}$ and $\sigma_{\min}$ are taken as average compressive stresses in the concrete (that is, half of the maximum stress at the extreme compressive fiber), and this can be computed based on elastic cracked section analysis. Equation (2) is applicable only if $\overline{\sigma_m} < 0.45$ and $\overline{\Delta\sigma} < 0.3$.

4.3 Deterioration in tensile stiffening

During cyclic loading, the concrete between the cracks is subjected to tensile fatigue which will lead to a progressive reduction in tensile stiffening of concrete. This progressive deterioration could be accounted for using the reduced cycle-dependent modulus of rupture[5], given by:

$$f_{cr,N} = f_{cr}\left(1 - \frac{\log_{10}N}{10.954}\right) \tag{5}$$

where f_{cr} = initial modulus of rupture of concrete, and $f_{cr,N}$ = modulus of rupture of concrete after N cycles of loading.

4.4 Cyclic softening of FRP in tension

Cyclic loading results in the degradation in stiffness of FRP laminates, which is accounted for by Ogin et al.'s model[7], that is:

$$E_{frp,N}/E_{frp} = 1 - [(p+1)q]^{1/(p+1)}(\sigma_{frp}/E_{frp})^{2p/(p+1)}N^{1/(p+1)} \tag{6}$$

where $E_{frp,N}$ = modulus of elasticity of FRP laminate after N cycles of loading, E_{frp} = initial modulus of elasticity of FRP laminate, σ_{frp} = maximum stress in FRP laminate, and p and q = empirical constants. The constant p indicates the rate of stiffness degradation of FRP laminate whereas q is a function of the stress in the FRP laminate. The degradation in stiffness can be related to the increase in strain in FRP laminate by the following expression which gives the fatigue coefficient of FRP, $\varphi_{frp,N}$:

$$\frac{E_{frp}}{E_{frp,N}} = \frac{\varepsilon_{frp,N}}{\varepsilon_{frp}} = \varphi_{frp,N} \tag{7}$$

where ε_{frp} = strain in FRP laminate before the start of cyclic loading, and $\varepsilon_{frp,N}$ = strain in FRP laminate after N cycles. From Eqs. (6) and (7), $\varphi_{frp,N}$ can be expressed as:

$$\varphi_{frp,N} = [1 - \{(p+1)q\}^{1/(p+1)}(\sigma_{frp}/E_{frp})^{2p/(p+1)}N^{1/(p+1)}]^{-1} \tag{8}$$

4.5 Calculation of deflections

The maximum deflection of a simply supported, elastic beam of span length l under two symmetrical concentrated loads after N cycles of repeated loading is:

$$\Delta = \frac{Pa}{48E_{e,N}I_{e,N}}[3l^2 - 4a^2] \tag{9}$$

where P = total load, and a = shear span. The value of $E_{e,N}$ can be calculated from Eq. (1) while the effective moment of inertia after N cycles, $I_{e,N}$ is given, following Branson's[9] formula, as:

$$I_{e,N} = \left(\frac{M_{cr,N}}{M_a}\right)^3 I_g + \left[1 - \left(\frac{M_{cr,N}}{M_a}\right)^3\right] I_{cr,N} \le I_g \tag{10}$$

where M_a = applied moment, and $M_{cr,N}$ = cracking moment after N cycles which can be evaluated from elastic bending theory once $f_{cr,N}$ is known from Eq. (5). Also, I_g = moment of inertia of a

gross section which can be computed considering a transformed section, and $I_{cr,N}$ = moment of inertia of a cracked section after N cycles. For a cracked rectangular section, $I_{cr,N}$ can be expressed as:

$$I_{cr,N} = \frac{bx_N^3}{3} + nA_s(d - x_N)^2 + (n-1)A_s'(x_N - d') + \frac{n_{frp}b_{frp}t_{frp}^3}{3} + n_{frp}b_{frp}t_{frp}(h - x_N)^2 \quad (11)$$

where b, b_{frp} = width of beam and FRP laminate, respectively, x_N = neutral axis depth, $n = E_s/E_{e,N}$ = modular ratio of steel to concrete, and $n_{frp} = E_{frp,N}/E_{e,N}$ = modular ratio of FRP laminate to concrete, A_s and A_s' = total area of tensile and compressive bars, respectively, d and d' = distances from top compression-most face to the centroids of tensile and compressive bars, respectively, and t_{frp} = thickness of FRP laminate. The neutral axis depth, x_N, for a cracked section can be determined considering force equilibrium and strain compatibility for the mid-span section. Once the values of $I_{cr,N}$ and $M_{cr,N}$ are known, $I_{e,N}$ can be calculated from Eq (10). Then using $E_{e,N}$ and $I_{e,N}$ in Eq. (9), the beam deflection under cyclic loading can be calculated.

5. Test results and discussion

The effects of load range and FRP reinforcement ratio on the beam deflection, stiffness and strains under cyclic loading are examined using Series I and II beams, respectively. Also, the deflections of FRP-bonded beams under cyclic loading are predicted by the proposed analytical method and compared with the test results.

5.1 Deflections

5.1.1 Effect of load range

Beams C11, C12 and C13 with ρ_{frp} = 0.64% were subjected to cyclic loading with the minimum load level at 35% of P_0 and maximum load levels at 55%, 65%, and 75% of P_0, respectively. As the minimum load level is the same for all three beams, the deflections are compared at the minimum load level after predetermined cycle numbers in Fig. 4(a). As expected, the deflections were larger for larger load ranges. Compared to Beam C11, Beams C12 and C13 deflected 9% and 44% more, respectively after 525,000 cycles. Also, Beams C12a and C13a deflected 4% and 34% more, respectively compared to Beam C11a after 75,000 cycles at which the last recorded data was obtained for Beam C13a. Beam C13a failed after 126,095 cycles by flexural crack-induced FRP debonding probably due to the high load range. Last, Beam C22b deflected 16% more than Beam C21b after 525,000 cycles.

5.1.2 Effect of FRP reinforcement ratio

Figure 4(b) shows the effect of GFRP reinforcement ratio on the deflections of RC beams under cyclic loading. Compared to Beam C02 (ρ_{frp} = 0%), Beams C12 (ρ_{frp} = 0.64% with a corresponding increase in flexural strength of 19% over C02) and C22 (ρ_{frp} = 1.28% with a corresponding increase in flexural strength of 32% over C02) deflected 15% and 20% less, respectively, at the end of 525,000 cycles. This reduction in deflections in GFRP-bonded beams may be due to the lower creep effect in concrete in the compression zone compared to the beam without FRP laminates, and lesser degradation in the concrete in the tensile zone due to stress re-distribution between the GFRP laminate and the steel reinforcement.

The effectiveness of GFRP system in controlling deflection compared to its effectiveness in flexural strength enhancement can also be demonstrated by examining Beams C02 (ρ_{frp} = 0%), C12a (ρ_{frp} = 0.64%) and C22b (ρ_{frp} = 1.28%). At the end of 525,000 cycles, Beams C12a and C22b deflected only slightly

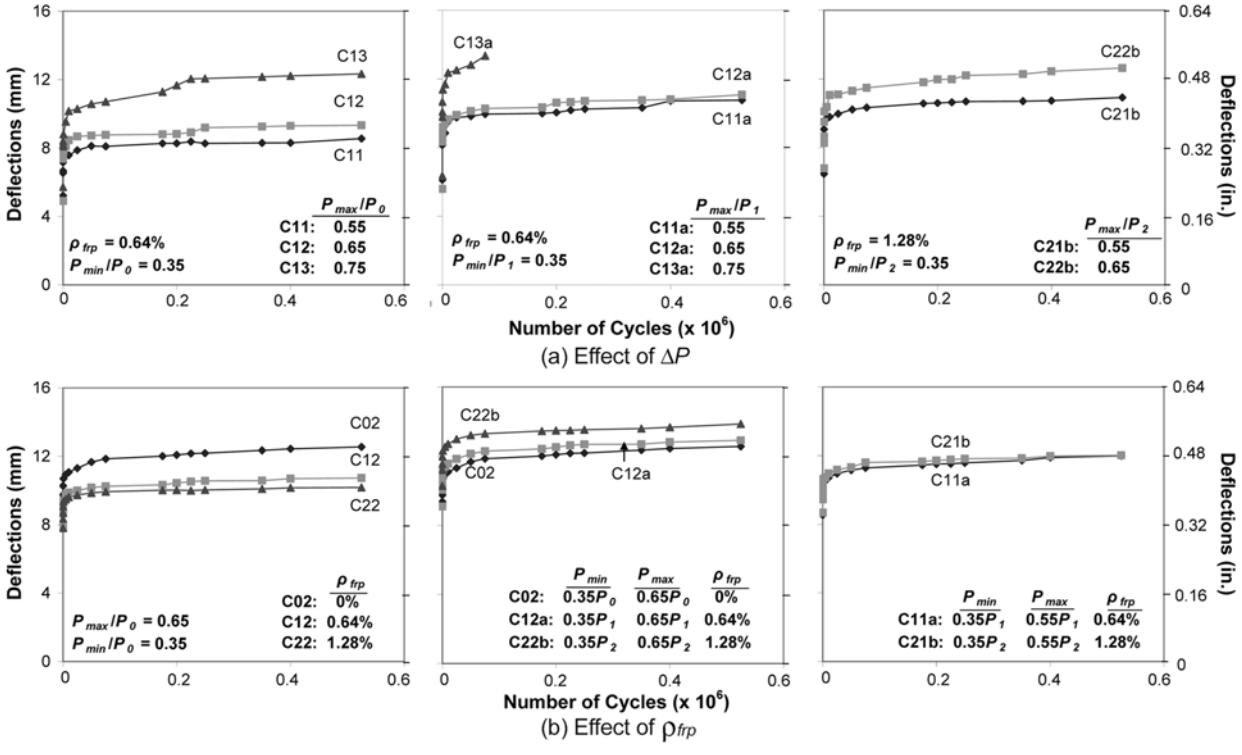

Fig. 4 Mid-span deflections.

more than Beam C02. Also, Beams C11a (ρ_{frp}= 0.64%) and C21b (ρ_{frp}= 1.28%) showed the same deflection at the end of 525,000 cycles. Therefore, under the same normalized load range, GFRP-bonded beams showed no significant difference from non-strengthened beams in terms of deflections.

5.2 Stiffness degradation

The degree of damage in beams can be measured from the degradation in stiffness at different cycles. The stiffness (EI) is computed by taking the slope of the load versus mid-span deflection curves. In the current investigation, the load-deflection curves (Figs. 5 and 6) for different number of cycles for all the beams seemed to remain linear. This is understandable as failure of the beams did not take place during the cyclic loading (except for Beam C13a). For Beam C13a, the last recorded data at 75,000th cycle did not show any sign of abrupt deterioration in stiffness that would have signified immediate failure. In general, the beams showed a gradual reduction in stiffness up to 100 or 1,000 cycles after which the reduction subsided. To compare the reduction in stiffness up to 1,000 cycles with respect to the 1st cycle, the normalized stiffness (EI_N/EI_0) curves are plotted in Fig. 7 for all beams.

5.2.1 Effect of load range

The stiffness curves for Series I beams are shown in Fig. 5. Beams C11, C12, and C13 (Fig. 7a) showed 4%, 26%, and 47% reduction in stiffness, respectively, after 1000 cycles compared to the 1st cycle. The same parameter for Beams C11a, C12a, and C13a is 3%, 15%, and 31%, respectively. The poorer performance of Beams C11, C12, and C13 may be due to the lower minimum load level, resulting in non-stabilization of existing cracks and increase in micro-cracking in concrete and subsequently more damage. As expected, Beam C22b, subjected to a larger load range, experienced more fatigue damage than Beam C21b.

5.2.2 Effect of FRP reinforcement ratio

Figure 6 shows the stiffness curves for Series II beams. The normalized stiffness versus number of cycles curves are plotted in Fig. 7(b) for these beams. The addition of GFRP laminate led to little improvement in stiffness for Beams C12 (6%) and C22 (7%) over Beam C02 after 1000 cycles. But Beams C12a and C22b showed a significant improvement of 21% and 25%, respectively in stiffness over C02. The poorer performance of Beams C12 and C22 is due to the lower minimum load level compared to Beams C12a and C22b, as explained earlier. In general, Beams C12a and C22b as well as C11a and C21b showed close relation in terms of stiffness. That is, beams when subjected to the same load ratio of their respective ultimate strength, showed the same stiffness. This implies that the GFRP laminates provide equal enhancement in strength and stiffness of the RC beam.

5.3 Strains in concrete, steel reinforcement bars and GFRP laminates

The strains in concrete, steel reinforcement bars and GFRPs at mid-span are shown in Figs. 8, 9, and 10, respectively. All the

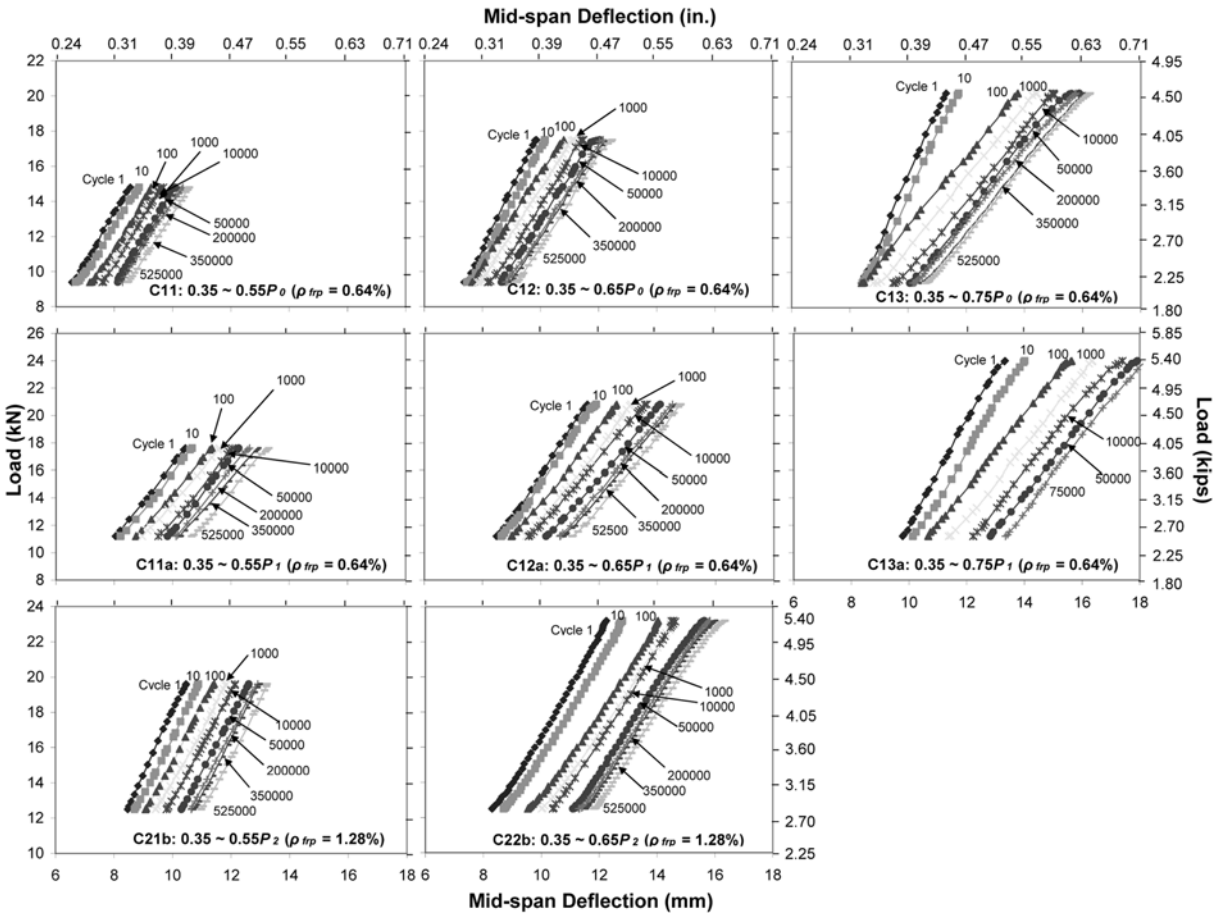

Fig. 5 Effect of load range on stiffness degradation.

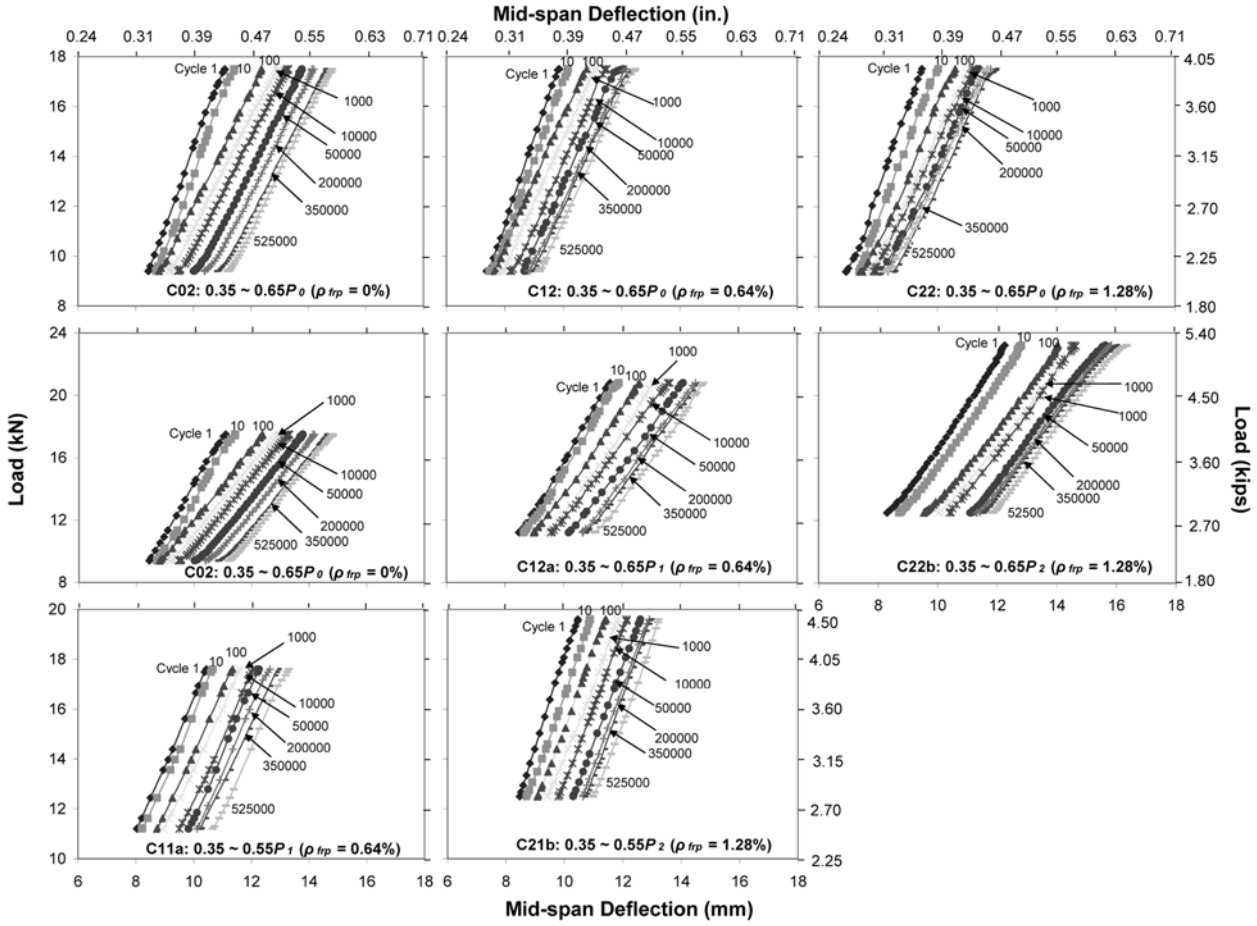

Fig. 6 Effect of FRP reinforcement ratio on stiffness degradation.

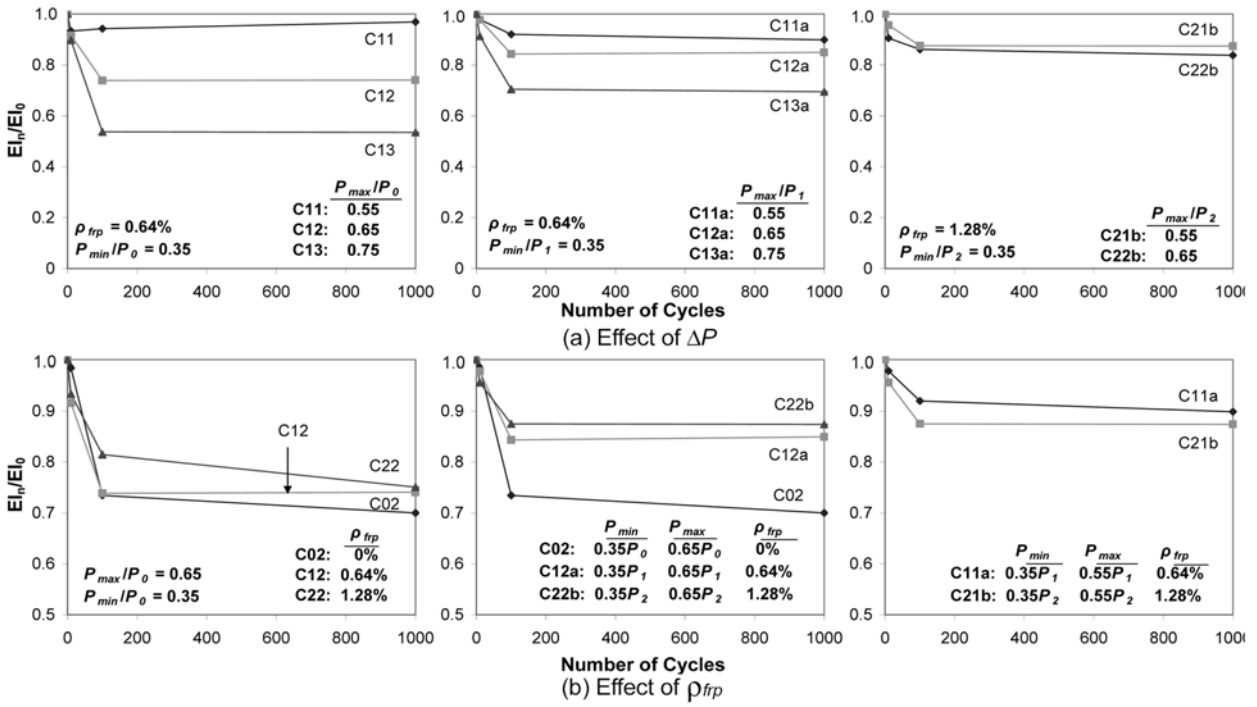

Fig. 7 Normalized stiffness.

strains are plotted in absolute values. For some beams (C13, C12a, and C22b), the plot for steel strains is terminated after several cycles as the strain gauges were spoiled. For Series I beams, the larger the load range, the higher was the strain. For Series II beams, the larger the FRP reinforcement ratio, the lesser was the strain. Beams C12 and C22 which were subjected to

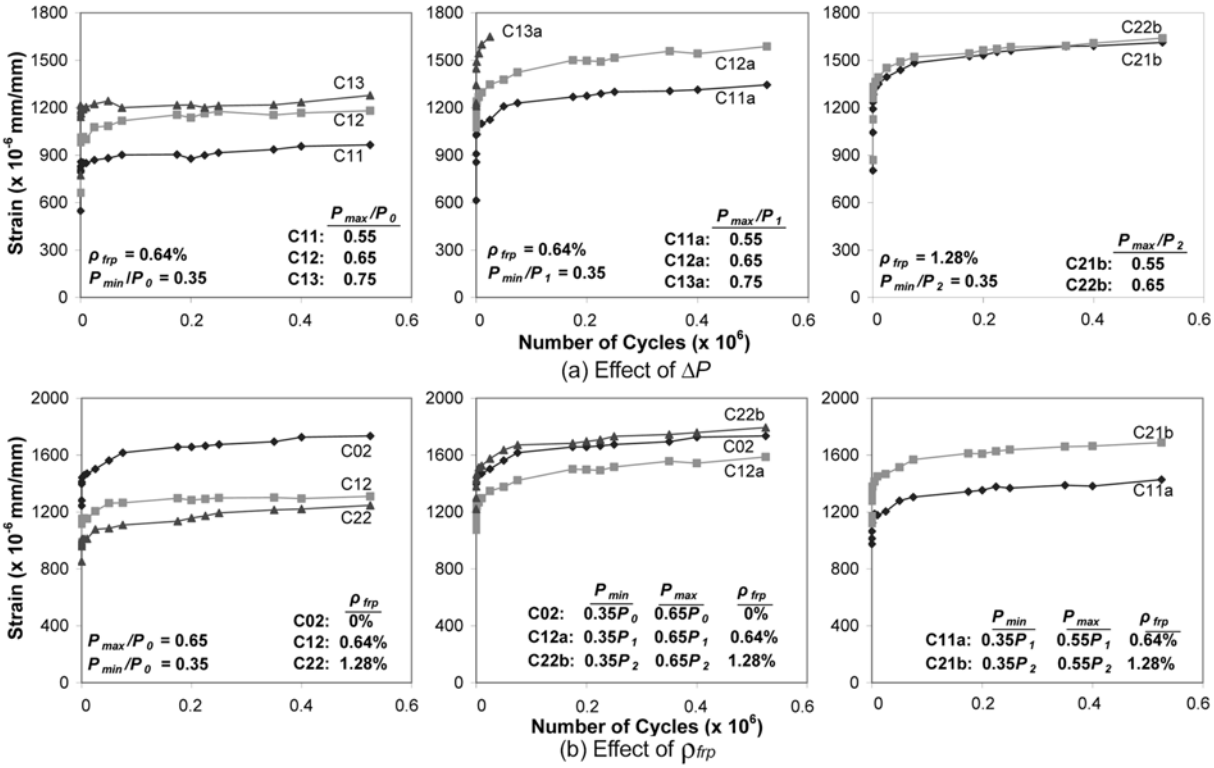

Fig. 8 Concrete strains at mid-span sections.

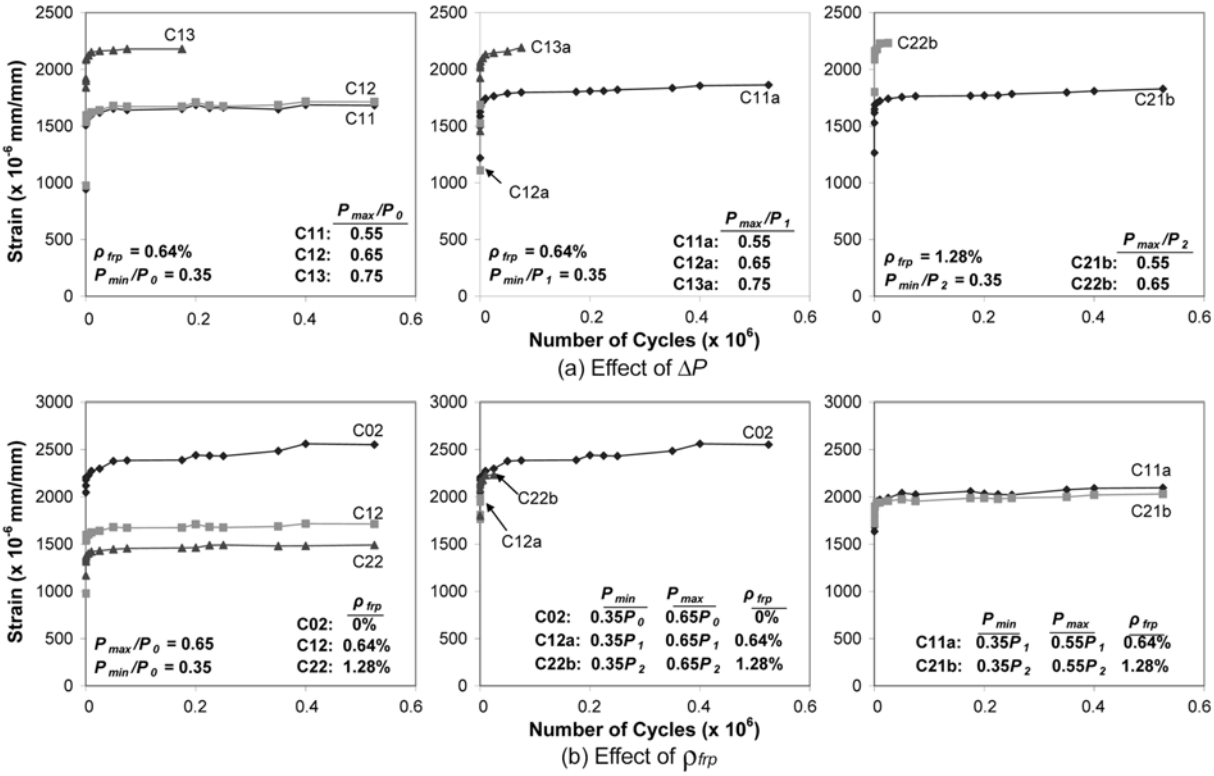

Fig. 9 Steel strains at mid-span sections.

loads between 35% and 65% of P_0, showed a maximum of 25% less strain in concrete and 42% less strain in steel bars, respectively than Beam C02. However, when the beams were subjected to the same load ratio of their respective static flexural strength, Beams C12a and C22b showed the same strains, but the strains were lesser than in Beam C02. Similarly, Beams C11a and C21b exhibited similar material strains in most of the cases except for concrete strains.

5. 4 Comparison with analytical approach

To compute the deflections of FRP-bonded RC beams under cyclic loading, the fatigue coefficients for FRP ($\varphi_{frp,N}$) need to be

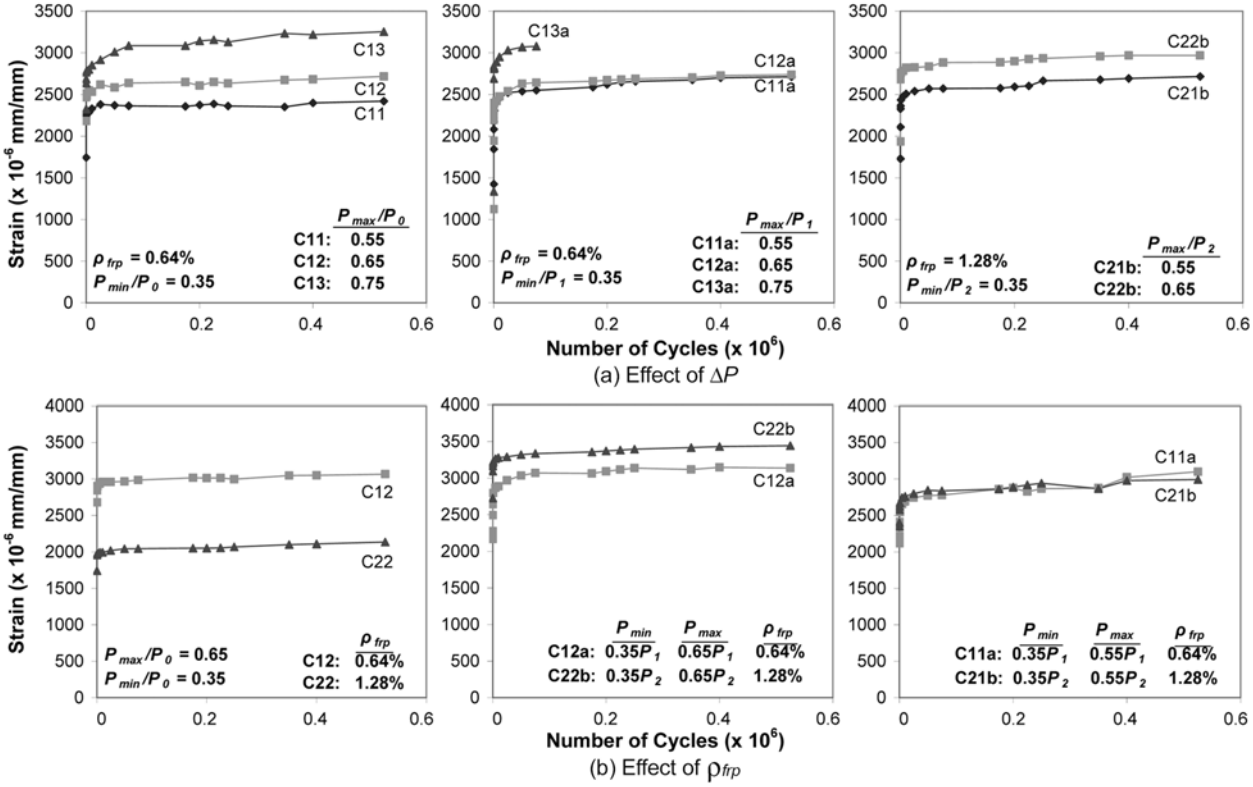

Fig. 10 FRP strains at mid-span sections.

known. It can be computed from Eq. (8) once the empirical constants, p and q are known. From fatigue tests conducted on GFRP coupons by Deskovic et al.[8], the values of p and q were established as 3.237 and 18.4×10^4, respectively. The glass fiber and resin used in fabricating the coupon had elastic modulus of 76 and 4 GPa respectively. The specimens were tested in different loading ranges from a minimum of 17 MPa to a maximum of 75 MPa at a frequency of 4.2 Hz. For the current experimental investigation, the properties of glass fiber and resin used in fabricating GFRP composite, and the applied loading range and frequency are close to those values used by Deskovic et al.[8].

Once the value of $\varphi_{frp,N}$ is known, the deflections are computed at mid-load levels for all the beams and compared with the test results in Fig. 11. The computed deflections in general, slightly under-estimated the actual ones including for the unstrengthened beam C02. This can be explained by the fact that the relation for the cyclic creep of concrete (Eq. 2) is applicable for $\overline{\sigma_m} < 0.45$ and $\overline{\Delta\sigma} < 0.3$. For most of the test beams, these parameters

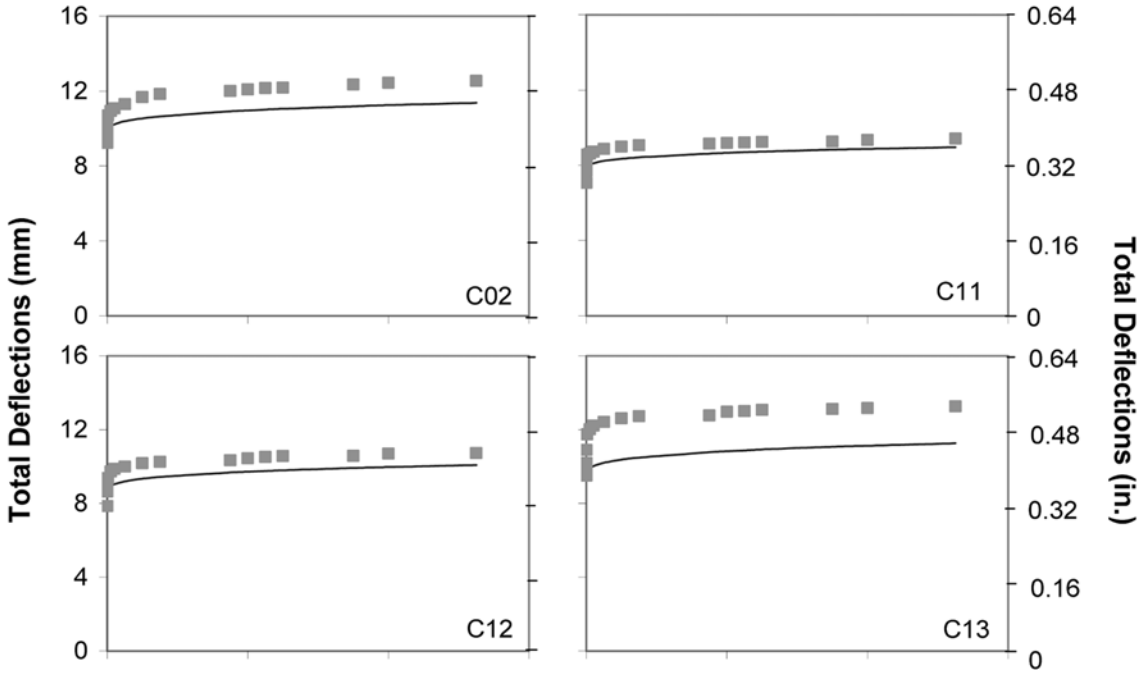

Fig. 11 Comparison of test results with analytical approach (continued)

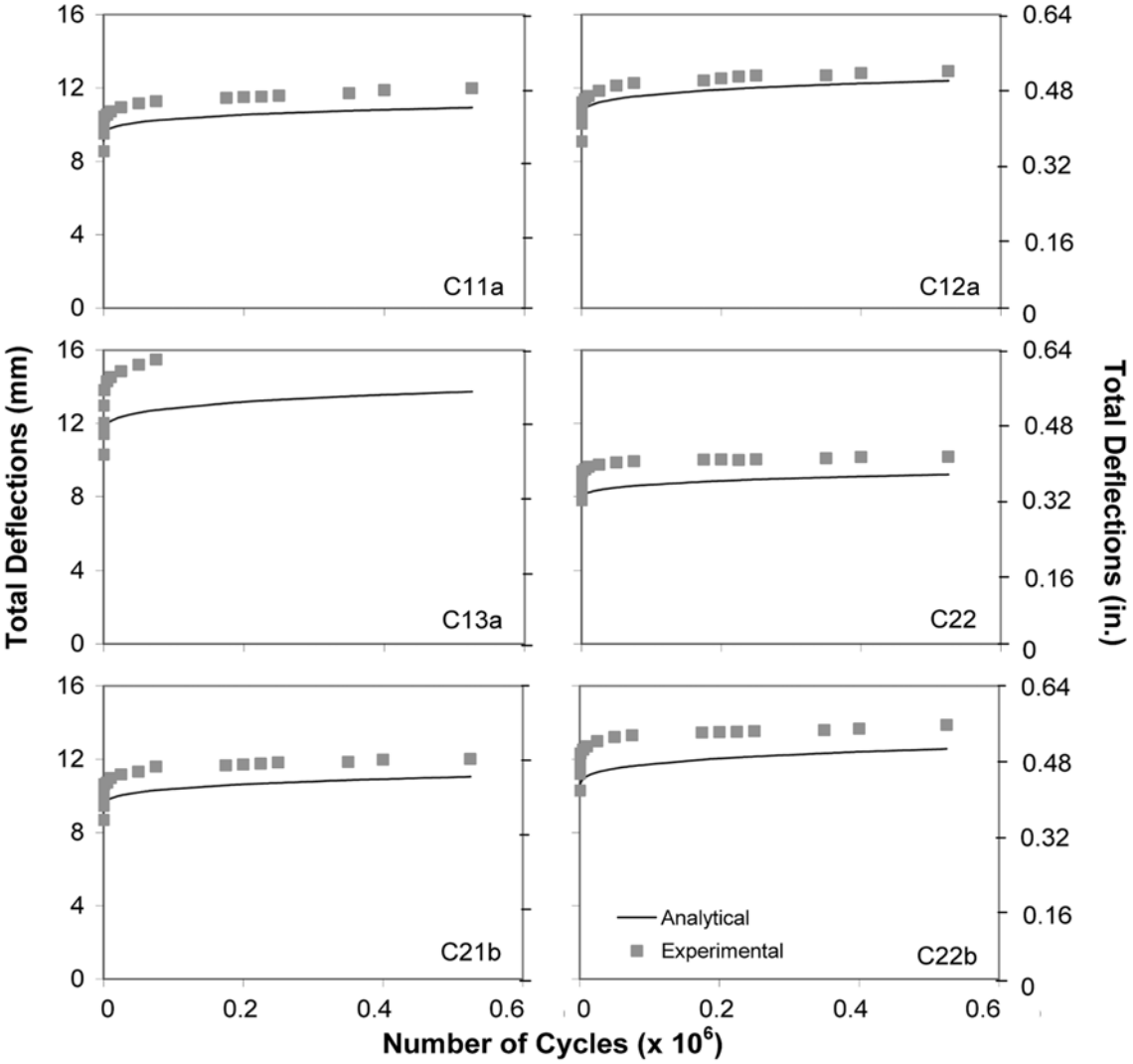

Fig.11 Comparison of test results with analytical approach.

either closely approached or exceeded the limiting values. In particular, Beams C13 and C13a did not meet both limiting criteria and were observed to exhibit about 15% and 18% larger deflections, respectively compared to the predictions at the end of 525,000 cycles.

6. Conclusions

From the investigation carried out, the following conclusions may be made:

1) GFRP laminates effectively control the deflections of RC beams under cyclic loading and its contribution towards controlling deflection is to the same extent as to flexural strength enhancement.

2) The stiffness of the beams under cyclic loading was found to degrade more with larger load ranges and lower minimum load level. GFRP laminates helped to reduce the degradation of stiffness due to cyclic loading.

3) The proposed analytical approach based on cycle-dependent effective moduli of elasticity of concrete and FRP laminate predicts the deflections of the test beams well and can be used for design purpose.

Notations

A_s, A_s' = total areas of tensile and compressive reinforcement bars, respectively

a = shear span of the beam

b, b_{frp} = width of beam and FRP cross-section, respectively

d, d' = distance of tensile reinforcement and compressive reinforcement bars from the top compressive surface of beam

$E_{e,N}$ = elastic modulus of concrete after N cycles

E_{frp}, $E_{frp,N}$ = elastic modulus of FRP laminate before and after N cycles, respectively

f_c' = concrete cylinder compressive strength at 28 days

f_{cr}, $f_{cr,N}$ = concrete modulus of rupture before and after N cycles, respectively

f_y, f_y' = yield strength of tensile and compressive reinforcement bars, respectively

$I_{cr,N}$ = moment of inertia of a transformed cracked section after N cycles

$I_{e,N}$ = effective moment of inertia after N cycles

I_g = gross moment of inertia of beam section

l = span of a simply supported beam

M_a = applied moment at section of maximum moment.

$M_{cr,N}$ = cracking moment after N cycles

n, n_{frp} = modular ratio of steel and FRP composite, respectively to concrete

p, q = experimental fatigue constants

P = total applied load on beam

P_{max}, P_{min} = maximum and minimum applied load during a load cycle

P_u = static flexural capacity of a beam.

P_0, P_1, P_2 = static flexural capacities of beams bonded without FRP, with one (1), and two (2) layers of FRP laminate, respectively

t = time after the beginning of cyclic loading in hours

t_{frp} = nominal thickness of FRP laminate

x_N = distance of neutral axis from top fiber after N cycles

ΔP = difference between maximum and minimum applied loads

$\overline{\Delta\sigma}$ = difference between average stresses determined at maximum and minimum load levels

$\Delta\sigma$ = stress range expressed as a fraction of static compressive strength

$\varepsilon_{c,N}$ = concrete strain after N cycles

ε_{frp}, $\varepsilon_{frp,N}$ = FRP laminate strain before and after N cycles at ultimate, respectively

ρ_{frp} = FRP reinforcement ratio

σ_{frp} = maximum stress in FRP laminate

σ_m, σ_{max}, σ_{min} = average stresses corresponding to mean, maximum and minimum applied loads, respectively

$\overline{\sigma_m}$ = average stress corresponding to mean applied load expressed as a fraction of static compressive strength.

$\varphi_{frp,N}$ = fatigue coefficient of FRP laminate

References

1. Heffernan, P. J. and Erki, M. A., "Fatigue Behavior of Reinforced Concrete Beams Strengthened with Carbon Fiber Reinforced Plastic Laminates," *Journal of Composites for Construction*, Vol.8, No.2, 2004, pp.132~140.

2. Shahawy, M. and Beitelman, T., "Static and Fatigue Performance of RC Beams Strengthened with CFRP Laminates," *Journal of Structural Engineering*, Vol.125, No.6, 1999, pp.613~621.

3. Breña, S. F., Benouaich, M. A., Kreger, M. E., and Wood, S. L., "Fatigue Tests of Reinforced Concrete Beams Strengthened Using Carbon Fiber-Reinforced Polymer Composites," *ACI Structural Journal*, Vol.102, No.2, 2005, pp.305~313.

4. Wu, Z. Y., Clement, J. L, Tailhan, J. L., Boulay, C., and Fakhri, P., "Static and Fatigue Tests on Precracked RC Beams Strengthened with CFRP Sheets," *6th International Symposium on Fiber-Reinforced Polymer Reinforcement for Concrete Structures (FRPRCS-6)*, Singapore, 2003, pp.913~922.

5. Balaguru, P. and Shah, S. P., "A Method of Predicting Crack Widths and Deflections for Fatigue Loading," *ACI Special Publication*, SP 75-7, 1982, pp.153~176.

6. Whaley, C. P. and Neville, A. M., "Non-Elastic Deformation of Concrete under Cyclic Compression," *Magazine of Concrete Research*, Vol.25, No.84, 1973, pp.145~154.

7. Ogin, S. L., Smith, P. A., and Beaumont, P. W. R., "A Stress Intensity Factor Approach to the Fatigue Growth of Transverse Ply Cracks," *Composites Science and Technology*, Vol.24, 1985, pp.47~59.

8. Deskovic, N., Meier, U., and Triantafillou, T. C., "Innovative Design of FRP Combined with Concrete: Long-Term Behavior," *Journal of Structural Engineering*, Vol.121, No.7, 1995, pp.1079~1089.

9. Branson, D. E., *Deformation of Concrete Structures*, McGraw-Hill, New York, 1977.